Platform for Measurements of the Casimir Force between Two Superconductors

Norte, R. A.; Forsch, M.; Wallucks, A.; Marinković, I.; Gröblacher, S.

DOI
10.1103/PhysRevLett.121.030405

Publication date
2018

Document Version
Final published version

Published in
Physical Review Letters

Platform for Measurements of the Casimir Force between Two Superconductors

R. A. Norte,* M. Forsch, A. Wallucks, I. Marinković, and S. Gröblacher†
Department of Quantum Nanoscience, Kavli Institute of Nanoscience, Delft University of Technology, Lorentzweg 1, 2628CJ Delft, The Netherlands

(Received 20 March 2018; published 20 July 2018)

Several experimental demonstrations of the Casimir force between two closely spaced bodies have been realized over the past two decades. Extending the theory to incorporate the behavior of the force between two superconducting films close to their transition temperature has resulted in competing predictions. To date, no experiment exists that can test these theories, partly due to the difficulty in aligning two superconductors in close proximity, while still allowing for a temperature-independent readout of the arising force between them. Here we present an on-chip platform based on an optomechanical cavity in combination with a grounded superconducting capacitor, which overcomes these challenges and opens up the possibility to probe modifications to the Casimir effect between two closely spaced, freestanding superconductors as they transition into a superconducting state. We also perform preliminary force measurements that demonstrate the capability of these devices to probe the interplay between two widely measured quantum effects: Casimir forces and superconductivity.

DOI: 10.1103/PhysRevLett.121.030405

The Casimir force can be interpreted as a direct consequence of the quantization of the electromagnetic field. It was first postulated by Casimir [1,2] in 1948 and conclusively experimentally observed by Lamoreaux in 1997 [3]. As two conducting plates are placed at a small distance from one another, an attractive force manifests between them. The effect was originally suggested to result from quantum vacuum fluctuations, while later derivations by Lifshitz explain its emergence from charge fluctuations in the conductors [4]. While the Casimir effect has been tested with various metallic and dielectric systems, it remains an open question how the force behaves between closely spaced surfaces as they transition into a superconducting state. It is known that superconductivity affects the reflectivity of a metal at frequencies below $k_B T_c/\hbar$ and that it should also change how the magnitude of the Casimir force depends on the temperature above and below the superconducting transition temperature T_c [5–8]. By experimentally determining these corrections around T_c, it should be possible to distinguish between competing descriptions of the frequency response of superconductors, such as the Drude and plasma models, as appropriate descriptions for the TE zero mode in calculations of the Casimir effect [9]. In addition, measuring the force arising between two superconductors could allow us to test recent proposals of a potential gravitational Casimir effect [10,11].

One of the main obstacles for such Casimir experiments has been the difficulty to realize small gaps between the surfaces of two objects at low temperatures [12,13]. Sophisticated nanopositioning systems are typically required to place the two objects tens of nanometers apart. While scanning tunneling microscopes can commonly achieve subnanometer spacings between a tip and a surface at a single atomic point, this type of proximity becomes difficult over the large surfaces and small gap sizes required to probe a measurable Casimir force. Many experiments have therefore used a sphere close to a plate for easier alignment (sphere-plate geometry), which significantly reduces the force compared to the original proposal of using two parallel plates. In addition, robust detection systems are required to not only measure the forces between these objects, but also to modulate and stabilize the gap to nanometer precision [14–18].

Incorporating superconductors introduces a number of additional challenges. For example, realizing a stable force detection that operates over a large temperature range, ideally well above and below the T_c of a superconductor, is difficult. A recent experiment using an electromechanical system was able to infer the Casimir force exclusively below T_c, where a superconducting LC (L stands for inductor and C for capacitor) readout circuit operates without significant losses [19]. It is also crucial that the force detection does not compromise the superconductivity of the films through additional heating by optical absorption, magnetic fields, or currents from measurements. Verifying that the entire structure is superconducting requires an integrated way to monitor the plates' resistance.

Here we realize a novel on-chip optomechanical sensor that allows us to optically measure the changes in the force between two plates made of superconducting material at any temperature, in particular while they are cooled through T_c. By engineering the entire superconducting structure and nanophotonic detection system on chip, we realize a versatile measurement platform that can be readily used

inside a dilution refrigerator at milli-Kelvin temperatures. The integrated photonic crystal microcavities allow us to measure modifications to the Casimir force before and after the onset of superconductivity with a resolution of 6 mPa between the surfaces. We have developed new fabrication methods that utilize high-stress films to realize state-of-the-art parallelism between freestanding superconducting surfaces over long distances without active stabilization. Our platform also has on-chip circuitry, which we use to accurately determine the superconductors' properties such as resistance, penetration depth, and coherence length. The optical force detection is stable at low temperatures, easily coupled using fiber optics, and operates at all temperatures without compromising the superconductivity of the films.

A generic schematic of our experiment is shown in Fig. 1(a). It consists of two parallel plates of a superconductor, which we choose to be aluminum. One of these plates is attached to the movable mirror of an optomechanical cavity. We monitor the resistance of the superconducting plates using a four-point measurement as they are cooled below their superconducting transition temperature T_c. Any temperature-dependent forces will affect the distance between the plates, causing an effective change in the length of the cavity and a shift in the cavity resonance frequency ω_c.

We realize an optomechanical system equivalent to the sketch in Fig. 1(a) by etching a photonic crystal cavity into two adjacent, high-stress (1.3 GPa) LPCVD silicon nitride

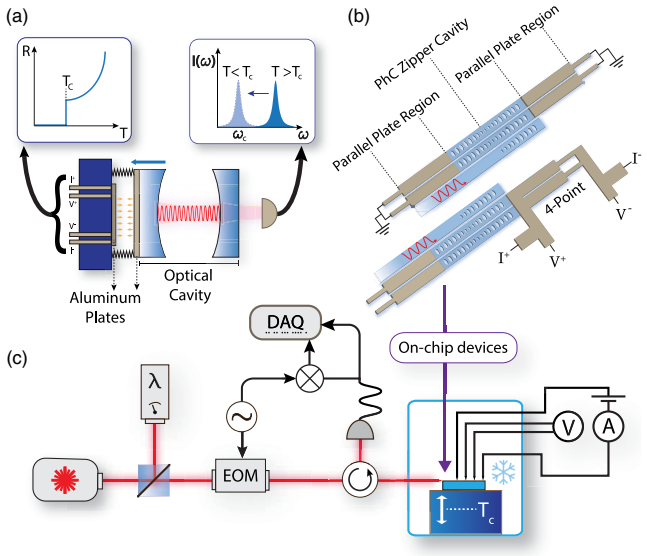

FIG. 1. (a) Working principle of the platform: The movable mirror of an optomechanical cavity is coated with an aluminum film and positioned in close proximity to a fixed aluminum plate. Any forces that arise between the plates at the onset of superconductivity would change the position of the movable mirror, which can be measured through a shift in the optical cavity resonance. (b) Illustration of our on-chip implementation of (a). We design a zipper cavity made of silicon nitride and evaporate aluminum on its support strings. By evanescently coupling light through a waveguide to the cavity, we can monitor its resonance frequency as a function of temperature. The resistance of the film is continuously probed through an additional device on the chip that is connected to a four-point measurement (bottom), allowing us to determine its T_c. (c) Sketch of the setup. We stabilize our laser to the resonance of the optomechanical cavity using a wavelength meter. The resonance frequency is monitored through a phase measurement by modulating sidebands onto the light field using an electro-optical modulator (EOM), which are detected, mixed down, and then digitized. The sample itself is mounted in a dilution refrigerator, where we can ramp the temperature above and below T_c, while monitoring its resistivity with the four-point measurement.

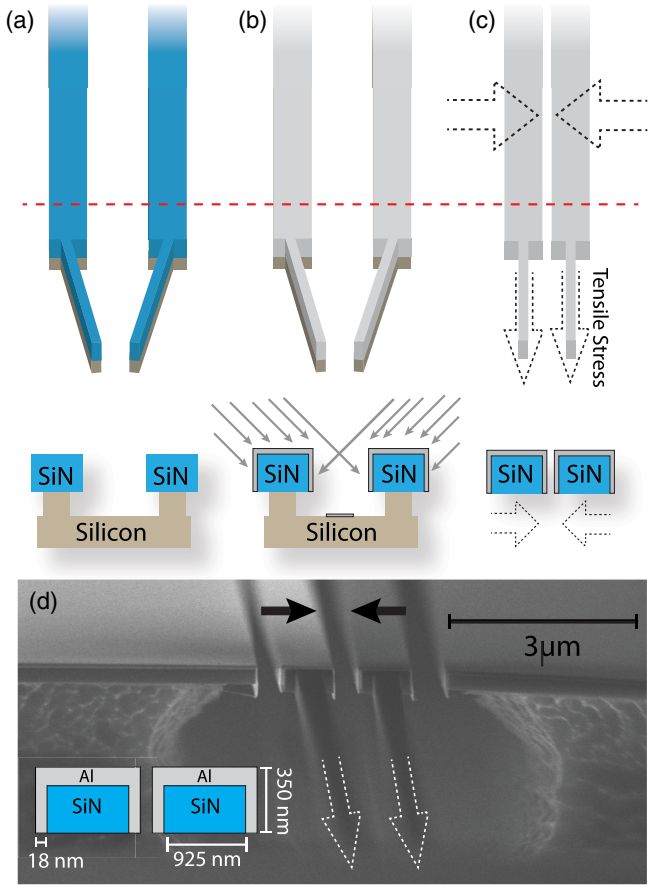

FIG. 2. We highlight how tensile stress in the SiN films is utilized to achieve small gaps between parallel superconducting plates over long distances. The bottom insets show the corresponding cross section through the top nanobeams (indicated by the red dashed line). (a) First, nanobeams are etched into the SiN film and into the Si substrate underneath. (b) Aluminum is then evaporated onto the nanobeams at two different angles to homogeneously cover the beams on its sides in order to form plates. (c) After the Si underneath the SiN is removed, the beams are free to move. The tensile stress in the SiN pulls the strings straight and taut. This simultaneously moves the nanobeams closer together, forming small gaps. The initial lithographically defined angle determines the gap size. (d) Side-view SEM image showing the profile of the metal that makes up the plates for the measurements. Here we show a device designed to have a 300 nm gap once suspended. The inset shows a cross section of the metallized portions of the nanobeams.

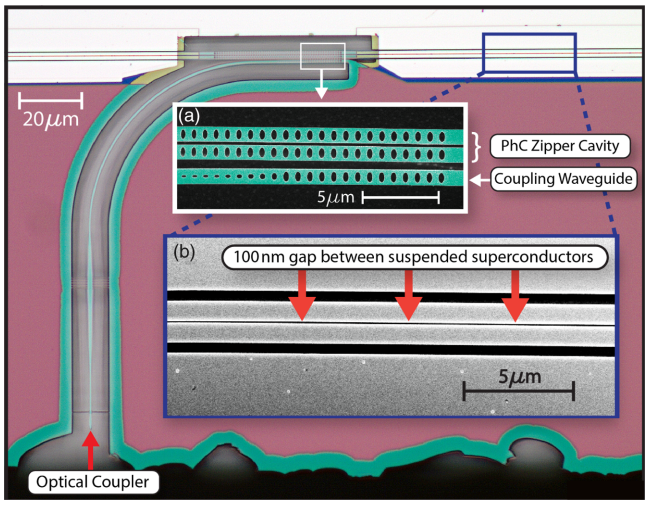

FIG. 3. Microscope image of a zipper cavity with integrated superconducting strings. In the lower left corner is an adiabatic coupler used to couple light from a lensed fiber to a waveguide, which is then evanescently coupled to the suspended photonic crystal zipper cavity. A close-up of this nanophotonic structure is shown in inset (a), where the reflector at the end of the waveguide is clearly visible, which allows us to send the reflected laser light back into the fiber. Inset (b) is a scanning electron microscope image of a section of the 170 μm suspended nanostrings, which are partially covered in aluminum and which, due to the large tensile stress in the silicon nitride film, are almost perfectly parallel with a gap of only 100 nm.

(SiN) beams, usually referred to as a zipper cavity [20] [see Figs. 1(b), 2, and 3 for more details]. Any relative motion between the two beams results in a shift of the optical cavity frequency ω_c. Suspending the photonic crystals are long tethers which connect to the substrate. The overall structure consists of two 384 μm-long parallel strings with a width $w = 926$ nm and thickness $t = 300$ nm. The large tensile stress allows the parallel beams to remain straight and closely spaced over long distances [21]. The tethers are partly covered with an aluminum film, which forms a pair of parallel plates. They are deposited with an 18 nm effective thickness (the thickness of the aluminum deposited on the sides of the nanostrings) and surface area $A = 220\ \mu\text{m} \times 350$ nm [cf. inset in Fig. 2(d)]. Unlike conventional Casimir measurements, we realize a force measurement with lithographically defined gaps in order to avoid spurious heating of the superconducting film from actively stabilizing the gap size. This allows us to have several devices per chip, each with a different predetermined gap size, with an achievable gap as small as $\approx$100 nm.

In order to fabricate the devices, we first etch the nanobeam structures into the SiN films and then proceed to etch deeper into the silicon substrate to produce the profile seen in Fig. 2(a). The initial large spacing between the nanobeams is important for two reasons: First, it allows us to make straight and vertical sidewalls of the SiN using a directional plasma etch (CHF_3/O_2). Lithographically defining and etching small gaps can be prone to surface roughness and angled sidewalls, which can significantly limit the achievable gaps between the metallized beams. Second, the large gaps allow for enough space between the beams to homogeneously cover the sidewalls with aluminum using an angled-stage electron-beam evaporator [cf. Fig. 2(b)]. The Si below the beams is then removed using an SF_6 plasma release. Once free to move, the tensile stress in the beams pulls them straight and taut, simultaneously also pulling them closer together [Fig. 2(c)]. The final gap size between the beams is defined by the initial lithographic angle of the SiN tethers seen in Fig. 2(a). By sweeping the angle of these tethers over several devices, we can controllably realize a variety of gap sizes on a chip. These pull-in techniques allow us to engineer the high-tensile stress in SiN films to achieve excellent parallelism over long distances [21].

To avoid spurious shifts from capacitive forces and minimize the influence of patch potentials [22], all wires are grounded. At ambient temperatures, the initial gap between the nanostrings already includes the Casimir force. The zipper cavity is located in the center of the beam where the expected displacement is maximal. The optical measurement of the cavity's resonance frequency is done by coupling laser light through a lensed fiber to a waveguide that is brought into close proximity of the cavity and hence allows us to evanescently couple light in and out with a total efficiency of about 55% [see Fig. 1(b), the Supplemental Material [23], and Refs. [27,28] for details]. The light is then reflected back into the fiber, where we send it through an optical circulator and into a photodetector.

We also fabricate a reference device with the same dimensions, which allows us to perform four-point measurements of the aluminum wire resistance and hence accurately determine when the wires become superconducting using a low-current ($\approx\mu$A) source [see Fig. 1(b)]. The measurements are performed in a closed-cycle dilution refrigerator with a base temperature of 10 mK, allowing us to cool the aluminum well below its T_c of approximately 1.3 K. The actual critical temperature for our devices is measured to be slightly below 1 K [cf. Fig. 4(a)]—we attribute this deviation from the literature value of aluminum to our particular geometry, which features thin wires [29] and minimal thermal conductivity due to its freely suspended SiN support.

When we first cool the zipper cavities from room temperature to about 3 K, we observe a shift in the optical resonance of typically a few nanometers, which is due to the temperature-dependent refractive index and thermal contractions. Most of the shift happens above 10 K, and no further shift in resonance frequency is expected or observed below that temperature. This is due to both silicon nitride and aluminum having a coefficient of linear thermal expansion approaching zero at cryogenic temperatures [30]. At first, we measure the device that has its aluminum

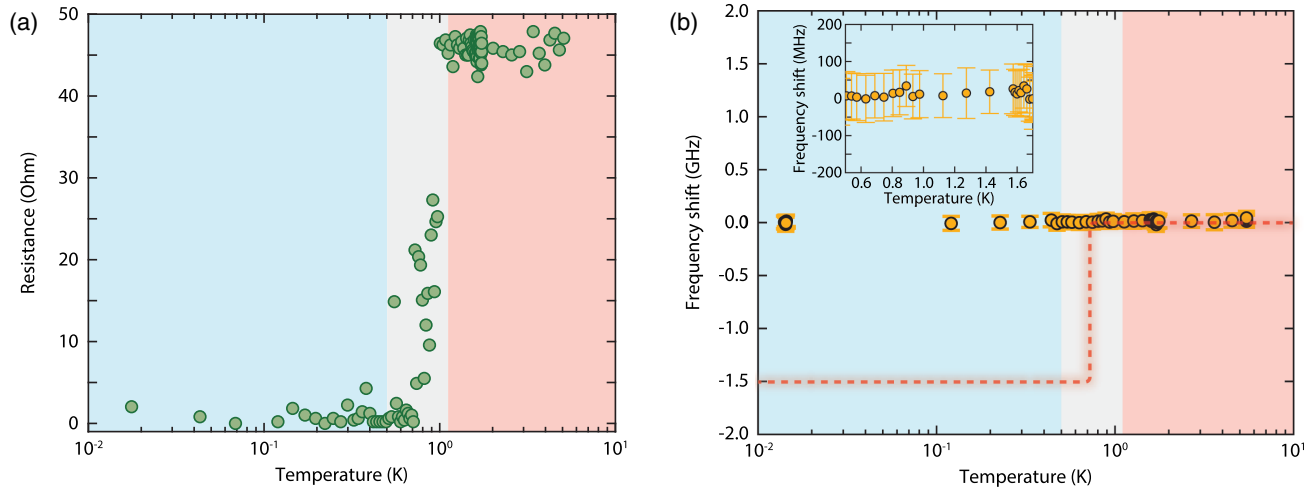

FIG. 4. (a) Shown is the resistance of the superconducting wires on our test device as a function of temperature. A jump from a few Ω to about 45 Ω is clearly visible just below 1 K. The data are collected from several four-point measurements using 1 μA of current, which results in a stable and very reproducible curve. The shaded regions are a guide to the eye, with blue representing the superconducting, gray the transition, and red the normal conducting state of the Al wire. (b) We plot the relative change in resonance frequency of the fundamental mode of a representative zipper cavity as a function of temperature. A force acting on the wires when they are in their superconducting state would shift the resonance frequency in the transition region between normal conductance and superconductance [see Fig. 1(a) for more details]. The gap size for this particular device is 100 nm (±10 nm, see the Supplemental Material [23]) with a measured optomechanical coupling rate of 50 GHz/nm. The red dotted line depicts the expected shift in frequency for a recently proposed gravitational Casimir experiment (see the text). The inset shows an overall variation in the central frequency of less than 30 MHz, mostly coming from variations and drifts in our measurement setup. Each data point is the average of 100 samples, and the error bars are shown in s.d.

wires connected to the four-point probe. At base temperature (10 mK), we continuously monitor the resistance as a function of the optical power sent into the zipper cavity. We use this measurement to choose a laser power for the actual measurements, 200 nW at the input of the dilution refrigerator, that is well below the threshold for the superconductivity to break down due to absorption of the laser and subsequent heating of the metal (∼1 μW).

We then perform measurements on several devices with gap sizes ranging from $a = 300$ nm down to just below $a = 100$ nm [for a sketch of the setup, see Fig. 1(c)]. The results for the bigger gaps do not deviate from the ones for the smaller gaps, and we will only focus on $a = 100$ nm, which should also exhibit the largest effects. The device used to obtain the data in Fig. 4(b) has a fundamental cavity resonance at $\lambda = 1586.3$ nm ($\omega_c \approx 2\pi \times 189$ THz) and a linewidth of $\kappa \approx \omega_c/Q_o = 2\pi \times 4.2$ GHz (optical quality factor of $Q_o = 4.5 \times 10^4$). We experimentally determine our coupling strength, which is the frequency shift of the cavity as a function of displacement, to be $g_{\mathrm{OM}}/2\pi \approx 50$ GHz/nm (see the Supplemental Material [23]), in good agreement with our simulated value of 50 GHz/nm. In our experiment we detect frequency shifts of the cavity resonance resulting form the Casimir force by measuring a phase shift using a Pound-Drever-Hall scheme [cf. Fig. 1(b) and the Supplemental Material [23] for details], with a minimally resolvable shift of 10 MHz (around 0.25% of the optical linewidth).

The state-of-the-art parallelism we have developed here gives us a minimal resolvable Casimir pressure of 6 mPa, corresponding to a gap change of the zipper cavity of a few hundred femtometers. When changing the temperature through the T_c of aluminum, we do not detect any frequency shift, as can be seen in Fig. 4(b). We repeat this measurement various times, with optical powers well below and above the critical power for the superconductivity to break down, and do not observe a shift. Our sensitivity already allows us to disprove the validity of a gravitational Casimir force predicted to occur between superconductors [10]. For our device, such forces are estimated to be 0.5 Pa, resulting in a cavity frequency shift of 1.5 GHz. One potential explanation for the absence of this Casimir force in our data is that the particular choice of our geometry could have a reducing effect on the force between the two superconducting wires. All our calculations are done for plates, which could in principle deviate from the actual geometry that we fabricate due to edge effects. In order to estimate the reductions in the Casimir pressure due to our parallel nanobeam geometry (compared to the infinite parallel plates), we turned to numerical calculations performed in [31] which use finite-difference time-domain methods [32,33] to calculate the Casimir force between two suspended rectangular beams at zero temperature—in good agreement with proximity force approximations [34] of the same geometries. For experiments testing the Casimir force with similar devices,

simulations and experiments have found the force to be about an order of magnitude smaller than the ideal plate-plate calculations [31]. However, the gravitational Casimir force would have to be about 2 orders of magnitude smaller than the large plates' calculation for it to be undetectable in our current measurement [see the inset in Fig. 4(b)].

To conclude, we have designed and fabricated on-chip optomechanical sensors that allow us to probe changes in the magnitude of the Casimir force between two superconductors. We are able to circumvent the conventional need for complex nanopositioning, stabilization, and force detection systems. Our versatile on-chip approach is easily integrable into a dilution refrigerator allowing us to stably probe for signatures of a change in the attractive force far below the T_c of aluminum. In our measurements we do not observe changes in the Casimir pressure to within our resolution of 6 mPa, which, with enhanced sensitivity, will allow us to determine the validity of the Drude and plasma models. These predictions strongly depend on the specific superconducting material, resulting in varying differential forces with respect to temperature [5–8]. In order to properly test these predictions, the noise performance and sensitivity of our devices could be improved by increasing the length of the tethers supporting the zipper cavity or alternatively by reducing the cavity linewidth or gap size further.

The techniques developed here offer new possibilities towards fundamental physics questions that have been out of reach for conventional experiments. It is an open question how the Casimir effect changes due to the type of superconductivity (i.e., type I, II, granular, crystalline, BCS, cuprate, high temperature etc.). Our chip-based approach is compatible with a number of thin-film materials including any superconductor that can be evaporated directionally onto a substrate. One interesting prospect would be to measure Casimir forces that arise between superconductors with higher T_c such as lead or cuprates such as BSCCO or YBCO. While van der Waals stiction at sufficiently small gap sizes is a serious limitation for electromechanical devices, the unique geometry of our devices allows us to reliably revive their functionality even after structural failure due to charging (see the Supplemental Material [23] for details). The high-aspect-ratio coupling between superconductors and optics developed here could also be interesting as an optomechanics platform aiming to perform quantum microwave-to-optics frequency conversion (i.e., coupling zipper cavities to a superconducting LC circuit) [35], which is currently a research field receiving significant attention.

We would like to thank Teun Klapwijk, Holger Thierschmann, Pieter de Visser, Andrea Caviglia, Giordano Mattoni, Alessandro Bruno, and Mark Ammerlaan for their support, as well as James Quach, Markus Aspelmeyer, Ralf Riedinger, Clemens Schäfermeier, Dirk Bouwmeester, Wolfgang Löffler, Kier Heeck, Galina Klimchitskaya, and Alexander Krause for stimulating and helpful discussions. This project was further supported by the European Research Council (ERC StG Strong-Q, Grant No. 676842), the Foundation for Fundamental Research on Matter (FOM) Projectruimte Grants (No. 15PR3210, No. 16PR1054) and by the Netherlands Organisation for Scientific Research (NWO/OCW), as part of the Frontiers of Nanoscience program and through a Vidi grant (Project No. 680-47-541/994).

*r.a.norte@tudelft.nl
†s.groeblacher@tudelft.nl

[1] H. B. G. Casimir and D. Polder, Phys. Rev. **73**, 360 (1948).
[2] H. B. G. Casimir, Proc. Kon. Ned. Akad. Wetensch. **51**, 793 (1948).
[3] S. K. Lamoreaux, Phys. Rev. Lett. **78**, 5 (1997).
[4] S. Lamoreaux, Phys. Today **60**, No. 2, 40 (2007).
[5] R. E. Glover and M. Tinkham, Phys. Rev. **108**, 243 (1957).
[6] G. Bimonte, E. Calloni, G. Esposito, L. Milano, and L. Rosa, Phys. Rev. Lett. **94**, 180402 (2005).
[7] G. L. Klimchitskaya and V. M. Mostepanenko, Phys. Rev. A **95**, 012130 (2017).
[8] H. Eerkens, Ph. D. thesis, Leiden University, 2017.
[9] G. Bimonte, Phys. Rev. A **78**, 062101 (2008).
[10] J. Q. Quach, Phys. Rev. Lett. **114**, 081104 (2015).
[11] E. Calloni, S. Caprara, M. DeLaurentis, G. Esposito, M. Grilli, E. Majorana, G. P. Pepe, S. Petrarca, P. Puppo, P. Rapagnani, F. Ricci, L. Rosa, C. Rovelli, P. Ruggi, N. L. Saini, C. Stornaiolo, and F. Tafuri, Nucl. Instrum. Methods Phys. Res., Sect. A **824**, 646 (2016).
[12] J. Laurent, H. Sellier, A. Mosset, S. Huant, and J. Chevrier, Phys. Rev. B **85**, 035426 (2012).
[13] R. Castillo-Garza, J. Xu, G. Klimchitskaya, V. Mostepanenko, and U. Mohideen, Phys. Rev. B **88**, 075402 (2013).
[14] B. W. Harris, F. Chen, and U. Mohideen, Phys. Rev. A **62**, 052109 (2000).
[15] R. S. Decca, D. Lopez, E. Fischbach, G. L. Klimchitskaya, D. E. Krause, and V. M. Mostepanenko, Ann. Phys. (Amsterdam) **318**, 37 (2005).
[16] H. B. Chan, Y. Bao, J. Zou, R. A. Cirelli, F. Klemens, W. M. Mansfield, and C. S. Pai, Phys. Rev. Lett. **101**, 030401 (2008).
[17] D. Garcia-Sanchez, K. Y. Fong, H. Bhaskaran, S. Lamoreaux, and H. X. Tang, Phys. Rev. Lett. **109**, 027202 (2012).
[18] J. Zou, Z. Marcet, A. W. Rodriguez, M. T. H. Reid, A. P. McCauley, I. I. Kravchenko, T. Lu, Y. Bao, S. G. Johnson, and H. B. Chan, Nat. Commun. **4**, 1845 (2013).
[19] R. Andrews, A. Reed, K. Cicak, J. D. Teufel, and K. W. Lehnert, Nat. Commun. **6**, 10021 (2015).
[20] A. G. Krause, T. D. Blasius, and O. Painter, arXiv:1506.01249.
[21] R. A. Norte, Ph. D. thesis, California Institute of Technology, 2014.
[22] C. C. Speake and C. Trenkel, Phys. Rev. Lett. **90**, 160403 (2003).
[23] See Supplemental Material at http://link.aps.org/supplemental/10.1103/PhysRevLett.121.030405 for more details, which includes Refs. [24–26].

[24] A. G. Krause, Ph. D. thesis, California Institute of Technology (2015).
[25] E. D. Black, Am. J. Phys. **69**, 79 (2001).
[26] U. Mohideen and A. Roy, Phys. Rev. Lett. **81**, 4549 (1998).
[27] S. Gröblacher, J. T. Hill, A. H. Safavi-Naeini, J. Chan, and O. Painter, Appl. Phys. Lett. **103**, 181104 (2013).
[28] R. Riedinger, S. Hong, R. A. Norte, J. A. Slater, J. Shang, A. G. Krause, V. Anant, M. Aspelmeyer, and S. Gröblacher, Nature (London) **530**, 313 (2016).
[29] J. Romijn, T. M. Klapwijk, M. J. Renne, and J. E. Mooij, Phys. Rev. B **26**, 3648 (1982).
[30] F. Pobell, *Matter and Methods at Low Temperatures*, 3rd ed. (Springer, Verlag, Berlin, Heidelberg, 2007).
[31] W. H. P. Pernice, M. Li, D. Garcia-Sanchez, and H. X. Tang, Opt. Express **18**, 12615 (2010).
[32] A. W. Rodriguez, A. P. McCauley, J. D. Joannopoulos, and S. G. Johnson, Phys. Rev. A **80**, 012115 (2009).
[33] A. P. McCauley, A. W. Rodriguez, J. D. Joannopoulos, and S. G. Johnson, Phys. Rev. A **81**, 012119 (2010).
[34] B. Derjaguin, I. Abrikosova, and E. Lifshitz, Q. Rev. Chem. Soc. **10**, 295 (1956).
[35] J. Bochmann, A. Vainsencher, D. D. Awschalom, and A. N. Cleland, Nat. Phys. **9**, 712 (2013).